

# The Myosin Catalytic Domain Does Not Rotate During the Working Power Stroke

Liang Zhao,\* Edward Pate,<sup>‡</sup> Anthony J. Baker,\* and Roger Cooke\*

\*Department of Biochemistry and Biophysics and Cardiovascular Research Institute, University of California, San Francisco, San Francisco, California 94143, and <sup>‡</sup>Department of Pure and Applied Mathematics, Washington State University, Pullman, Washington 99164

**ABSTRACT** Electron paramagnetic resonance spectroscopy of a spin probe attached to cys-707 on myosin cross-bridges was used to monitor the orientation of the myosin catalytic domain at the beginning and end of the working power stroke in active muscle. Elevated concentrations of orthophosphate and decreased pH were used to shift the population of cross-bridges from force-producing states into low force, pre-power-stroke states. The spectrum of probes in active fibers was not changed by conditions that reduced tension by 70%, indicating that the orientation of the catalytic domain was the same at the beginning and end of the power stroke. Thus the data show that the catalytic domain remains rigidly oriented on the actin filament during the power stroke.

## INTRODUCTION

The force and motion produced by contracting muscle results from a cyclic interaction between the contractile proteins, actin and myosin. In this cycle a myosin cross-bridge attaches to an actin filament and produces a power stroke in which the actin filament is translated by approximately 10 nm. This translation is thought to result from conformational changes within the myosin head (reviewed in Cooke, 1986; Goldman, 1987). A fundamental, unresolved question in muscle biophysics concerns the nature of the structural changes that occur within the myosin cross-bridge during the working power stroke. These were originally thought to involve a rotation of the entire myosin head, which acted as a rowing oar. However, more recent structural studies, discussed below, suggest that a portion of the myosin head is oriented rigidly on the actin filament during the power stroke, while a second region acts as the rowing oar.

The recent x-ray crystallographic solution of myosin subfragment-1 (S1) and the derived structure of S1 bound to F-actin have brought renewed impetus to this question (Rayment et al., 1993a,b; Schroder et al., 1993). The structure of S1 consists of a large globular region (the catalytic domain) that contains sites for binding both actin and nucleotide. Extending from this globular region is a long (85 Å) neck region that ends in the junction with the myosin thick filament. These structures have suggested a model for force production in which the catalytic domain of myosin is thought to attach in a rigid fashion to actin (Rayment et al., 1993a). Subsequent opening of the nucleotide pocket, mediated by nucleotide hydrolysis and release of the  $\gamma$ -phosphate of ATP, results in a change in the orientation of the

neck region. The neck then functions as a lever arm, producing a 5- to 10-nm power stroke. A central tenet of this hypothesis, that the catalytic domain should remain rigidly oriented on actin during the power stroke, can thus be tested by comparing the orientations of the catalytic domain at the beginning (pre-power-stroke) and at the end (post-power-stroke) of the working cycle. The post-power-stroke state is the well defined, rigor state. However, the structure of the physiological pre-power-stroke state remains undefined. We address this uncertainty here.

A number of lines of evidence from both biochemical and mechanical studies have supported the pivotal role of  $P_i$  release in the initiation of the working power stroke (reviewed in Hibberd and Trentham, 1986; Cooke, 1986; Goldman, 1987; Hibberd et al., 1985). The initial attachment of cross-bridges to actin is thought to be in a low force, weakly attached, pre-power-stroke  $A \cdot M \cdot ADP \cdot P_i$  state (A for actin; M for myosin) that is in equilibrium with a similar  $A \cdot M \cdot ATP$  state.  $P_i$  release from the pre-power-stroke cross-bridge then results in a transition to a strongly bound, force-producing, post-power-stroke state. Of particular relevance is the observation that in fibers,  $P_i$  is able to rebind to the myosin active site, reversing the low to high force transition and increasing the fraction of cross-bridges in the pre-power-stroke configuration. Mechanically, this is observed to depress isometric tension. However, fiber stiffness decreases less than force, indicating that a fraction of the pre-power-stroke cross-bridges remain attached to actin (Hibberd and Trentham, 1986; Cooke, 1986; Goldman, 1987; Hibberd et al., 1985). The effects of increased  $[H^+]$  on fiber mechanics are similar to those of increased  $[P_i]$ , with tension inhibited more than stiffness (Metzger and Moss, 1987, 1990; Renaud et al., 1987; Cooke et al., 1988; Seow and Ford, 1993; Fitts, 1994). This may suggest that decreased pH also increases the fraction of pre-power-stroke cross-bridges. The myosin hydrolysis step is inhibited at the lower pH (Taylor, 1977), also suggesting that the states populated may precede the power stroke and include

Received for publication 1 December 1994 and in final form 6 June 1995.

Address reprint requests to Dr. Roger Cooke, Department of Biochemistry and Biophysics, Cardiovascular Research Institute, University of California, San Francisco, San Francisco, CA 94143. Tel.: 415-476-4836; Fax: 415-476-1902; E-mail: COOKE@GCL.UCSF.EDU.

© 1995 by the Biophysical Society

0006-3495/95/09/994/06 \$2.00

A·M·ATP. Thus in our study we employed, singly and in combination, increased  $[P_i]$  and decreased pH ( $7 \rightarrow 6.2$ ) to preferentially populate the pre-power-stroke cross-bridge state. A further motivation for the study of decreased pH was that at low pH the singly charged, diprotonated phosphate species predominates in solution ( $pK_a = 6.8$ ). Hence, we could maintain constant solution ionic strength while using a 25% higher  $[P_i]$ .

## MATERIALS AND METHODS

Rabbit psoas fibers were chemically skinned and mechanical measurements were made using previously described protocols (Cooke et al., 1988). The reactive sulfhydryl cys-707 (SH-1) of myosin in glycerinated rabbit psoas fibers was labeled with *N*-[1-oxyl-2,2,6,6-tetramethyl-4-piperidinyl] maleimide (MSL) using a procedure described in detail by Zhao et al., (1995). Small bundles of 25–50 skinned fibers were washed in 20 mM MOPS, 5 mM  $MgCl_2$ , 1 mM EGTA, pH 7.0 (buffer A) for 20 min to remove the glycerol present in the skinning solution. The fibers were then incubated for 60 min in buffer A to which 60  $\mu M$  2–2'-dithio-bis(5-nitropyridine) ( $NO_2SPY$ ) had been added (pre-block step). Fibers were subsequently washed again in buffer A for 10 min, followed by a 10-min equilibration in 0.18 M KOAc, 5 mM  $MgCl_2$ , 5 mM EGTA, 20 mM MES, pH 6.5 (buffer B). Fibers were then labeled for 20 min in buffer B, with 0.1 mM MSL and 5 mM  $Na_4P_2O_7$  added. Fibers were subsequently washed for 10 min in buffer B to remove unreacted MSL labels and then equilibrated for 40 min in skinning buffer. All of the above steps were performed at 0°C. Fibers were then stored at  $-20^\circ C$  until use. Before experimentation, the fibers were washed with rigor buffer (see below) containing 5 mM dithiothreitol for 30 min.

The MSL-labeling steps above are similar to those described previously (Thomas and Cooke, 1980). The additional, pre-block step is carried out under conditions in which cys-707 is only weakly reactive, allowing  $NO_2SPY$  to form disulfide bonds with other SH groups in the fibers and hence blocking these groups from reacting with MSL during the labeling step. After the MSL labeling of cys-707, the disulfide bonds formed with  $NO_2SPY$  are removed by washing with dithiothreitol. This modification of the labeling protocol provided greatly enhanced specificity of labeling for cys-707, resulting in the labeling of 40–50% of myosin cys-707 in the fiber (Zhao et al., 1995). Thus, it was not necessary to react fibers with  $K_3Fe(CN)_6$  to reduce the EPR signal from nonspecific labeling as has sometimes been the practice in the past.

EPR measurements were performed with an ER/200D EPR spectrometer from Bruker Instruments (Billerica, MA). X-band, first-derivative absorption EPR spectra were obtained with the following setting: microwave power, 25 mW; gain,  $1.0 \times 10^6$ ; center field, 0.3475 Tesla; time constant, 100 ms; frequency, 9.74 GHz; modulation, 0.08–0.2 mTesla at a frequency of 100 kHz. The baselines for all spectra are 10.0 mTesla wide. Each spectrum used in data analysis represents the average of 20–40 distinct sweeps from an individual experimental preparation of ~100 spin-labeled fibers secured at constant length in a capillary aligned parallel to the magnetic field, in the center of the  $TE_{011}$  cavity. The sweep time was 10 s. Experimental buffer was flowed through the capillary at a rate of ~2 cm/s.

The measurements of single fiber mechanics were made by using the experimental apparatus described by Pate et al. (1994) and Zhao et al. (1995), which permits transferring mounted fibers between wells containing differing experimental buffers. Single fibers were dissected from a small bundle of glycerinated fibers and mounted in a well between a solid-state force transducer (Akers 801; SensoNor, Horten, Norway) and an arm connected to a rapid motor (General Scanning, Watertown, MA) for changing muscle length. Buffer was added to the well immersing the fiber. The length of mounted fiber was measured at  $\times 20$  magnification with the graticule of a dissecting microscope mounted directly over the fiber well. The resonant frequency of the transducer with mounted fiber was 2 kHz. Fiber tension was monitored by a 486 personal computer with Tecmar A/D

boards (Tecmar Co., Cincinnati, OH). Isometric tension was normalized with respect to fiber area by measuring the fiber diameter at five to seven locations along the fiber at  $\times 126$  magnification and averaging the values.

Fiber stiffness was determined from a series of rapid extensions of muscle length of differing magnitudes applied to a fiber. For these measurements, a 1% change in muscle length was 90% complete in 0.5 ms. This corresponds to a speed of stretch of  $2 \times 10^3$  nm/half-sarcomere/s. Fibers were typically stretched by 0.3, 0.6, 0.9, and 1.2% of fiber length, and the peak force was reached after the stretch was determined. The plot of peak force versus the percent length change was linear to a good approximation, and a least-squares linear fit was made to the data. The slope was taken as the fiber stiffness (Cooke et al., 1988). Although the stiffness was measured on single fibers and the spectra on bundles, this should not pose a problem. Measurements of stiffness on small bundles of three to five fibers provide values that are the same as for single fibers.

The experimental apparatus described above was used to study single fibers. To determine whether the changes found in the single fibers also occurred in the bundles of fibers observed in the EPR experiments, a second apparatus was constructed. Fibers were mounted in a capillary and perfused via a pump from one end, as in the EPR cell. The other end of the capillary was left open and the bundle was connected via surgical thread to a force transducer. Force was recorded as a series of relaxing or activating solutions perfused the fibers. The diameter of the bundle of fibers was measured at 7 to 10 locations along the bundle at  $\times 20$  magnification and values were averaged.

The experimental buffers for both EPR and mechanical experiments contained 5 mM MgATP, 30 mM creatine phosphate (CP), 5 mg/ml creatine phosphokinase (CK), 1 mM EGTA, and 20 mM MOPS (pH 7.0) or 20 mM MES (pH 6.2), with variable concentrations of potassium acetate,  $KH_2PO_4$ ,  $K_2HPO_4$ , and  $MgCl_2$ , maintaining a constant calculated ionic strength of 230 mM. For rigor conditions, ATP, CP, and CK were omitted. To activate fibers,  $CaCl_2$  was added, yielding a final pCa of ~4.5. As a result of  $P_i$  contamination in commercially available CP and ATP, buffers described as containing 0 added  $P_i$  contained ~1 mM  $P_i$ . Temperature was maintained at  $22^\circ C$  for all experiments.

## RESULTS

EPR spectroscopy has proven to be a powerful tool for monitoring the orientation of functioning muscle cross-bridges (Thomas and Cooke, 1980; Thomas, 1987). A maleimide spin label (MSL) can be rigidly attached to a highly reactive cysteine (cys-707) on the myosin head (Thomas and Cooke, 1980). Fig. 1 A shows the EPR spectrum of rigor, MSL-labeled fibers. The spectrum consists of three sharp lines that indicate an oriented population of probes. The splitting between the lines depends upon the angle between the magnetic field of the spectrometer and an axis within the probe. For the spectrum of rigor fibers in Fig. 1 A, the probes were highly ordered (a Gaussian distribution at an angle of  $82^\circ$  with respect to the fiber axis with a full width at half-maximum of  $12\text{--}15^\circ$ ). Fig. 1 B shows the spectrum observed when the rigor fibers in Fig. 1 A were relaxed, detaching myosin from actin. The three sharp lines were replaced by broadened peaks that were indicative of a highly disordered angular distribution of probes. Although the entire spectral widths were used in subsequent data analyses, the spectral change between the rigor and relaxed states was most easily observed from the decrease in the peak that originates from ordered probes ( $P_2$ ) and the concurrent increase in the peak originating from disordered probes ( $P_1$ ).

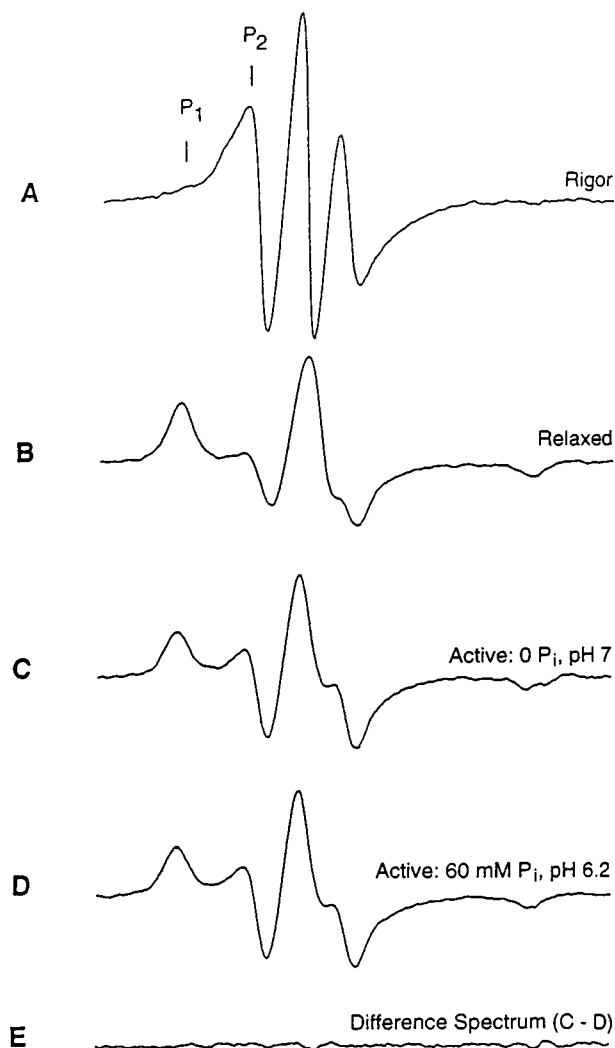


**FIGURE 1** EPR spectra from the same bundle of MSL-labeled fibers obtained in the following conditions. (A) Rigor. The spectrum consisted of three sharp lines indicating a highly ordered population of probes (Gaussian distribution angled at  $82^\circ$  to the fiber axis, with a full width at half-maximum of  $12\text{--}15^\circ$ ). (B) Relaxation. The three sharp lines were replaced by broadened peaks that were indicative of a highly disordered, isotropic angular distribution of probes after myosin detached from actin. (C) Activation, 0 added  $P_i$ , pH 7.0. (D) Activation, 60 mM  $P_i$ , pH 6.2. Spectrum E shows the difference between the spectra of fibers activated in 0 and 60 mM added  $P_i$  (C and D). There is no significant difference between the spectra in C and D, indicating that the orientation of the probes in active fibers was unchanged as the fraction of pre-power-stroke cross-bridges was increased by increased  $[P_i]$  and  $[H^+]$ . The spectra show the derivative of absorption as a function of the magnetic field, with a sweep width of 10 mTesla.

Previous studies of rigor and relaxed conditions have found spectra similar to those in Fig. 1 (Cooke et al., 1982; Fajer et al., 1990). Moreover, the probes in active fibers were previously found to be a linear combination of two distinct populations: one was ordered, with an orientation similar to that of rigor, and the other was disordered as in relaxation. Fig. 1 C shows the spectra obtained from active, isometric fibers for conditions in which the experimental

buffer contained 0 mM added  $P_i$ , pH 7.0. Similar to previous studies of active fibers, the increased ordering of probes in active fibers compared with relaxed fibers was evidenced by the increase of  $P_2$  in Fig. 1 C when compared with Fig. 1 B. To define the structure of pre-power-stroke cross-bridges, we also examined the orientation of the labeled muscle fibers at elevated  $[P_i]$ . Thus we used conditions that selectively increased the population of pre-power-stroke states. Fig. 1 D shows the spectra obtained for active contraction in a buffer containing 60 mM  $P_i$ , pH 6.2. The difference spectrum between Fig. 1, C and D, is given in Fig. 1 E. This spectrum is flat to within experimental error and indicates that there is no difference in either the percent of ordered probes present, or the angular orientation of the ordered component at low and high  $[P_i]$ . Table 1 gives the percentage of ordered probes, and the isometric tension and mechanical stiffness data for the active conditions described above. The increase in  $[P_i]$  from 0 to 60 mM and the decrease in pH from 7.0 to 6.2 caused a decrease of 70% in tension and 30% in stiffness. However, the fraction of ordered probes was  $\sim 19\%$  under both conditions. Thus our fundamental observation is that despite the large reduction in the population of strongly bound, force-producing cross-bridges in the presence of elevated  $[P_i]$ , the ordered fraction of cross-bridges monitored by EPR is the same at low and high  $[P_i]$ .

The ordered component of labeled fibers during active contraction is analyzed in greater detail in Fig. 2. Fig. 2 A is 0.20 times the rigor spectrum (Fig. 1 A). The solid line in Fig. 2 B is the spectrum of active fibers obtained at pH 7.0, 0 added  $P_i$  (Fig. 1 C) minus 0.80 times the relaxed spectrum (Fig. 1 B). The dashed line in Fig. 2 B is the equivalent difference for the active spectrum obtained at pH 6.2, 60 mM  $P_i$  (Fig. 1 D). The residual spectra from the fit to 20%

**TABLE 1** Mechanical parameters and EPR ordered fraction for active fibers at varying  $[P_i]$  and pH

	Tension (N/mm <sup>2</sup> )	Stiffness (N/mm <sup>2</sup> )	Ordered fraction (% rigor)
0 added $P_i$ , pH 7.0	$0.16 \pm 0.01$ (8)	$11.7 \pm 0.5$ (8)	$19.6 \pm 1.2$ (15)
0 added $P_i$ , pH 6.2	$0.10 \pm 0.01$ (10)	$10.7 \pm 0.4$ (10)	$19.2 \pm 1.4$ (4)
44 mM $P_i$ , pH 7.0	$0.09 \pm 0.01$ (10)	$9.5 \pm 0.4$ (10)	$18.0 \pm 2.7$ (4)
60 mM $P_i$ , pH 6.2	$0.05 \pm 0.01$ (10)	$8.2 \pm 0.3$ (10)	$19.1 \pm 1.3$ (15)

Mechanical and EPR properties of active fibers varying  $[P_i]$  and pH, singly and in combination. The measurements of active tension and stiffness were from MSL-labeled fibers taken from the same fiber bundles as used for EPR experiments. The relative ordered fractions in the EPR spectra were obtained by decomposition as shown in Fig. 2. Data are mean  $\pm$  SEM, with the number of observations shown in parentheses. Isometric tension was decreased by either an increase in  $[P_i]$  or by a decrease in pH, with smaller changes occurring in stiffness. However, the ordered component in the EPR spectrum was unchanged by any of the conditions. As in Fig. 2, C and D, all difference spectra were flat (spectra not shown). The proportional changes in tension and stiffness as a result of increased  $[P_i]$  were approximately the same at both pH 7.0 and pH 6.2, suggesting that the states populated by decreasing the pH resemble those populated by increasing  $[P_i]$  both structurally and mechanically. In addition, the data show that variation in pH does not affect our conclusions as regards variation in  $[P_i]$ .

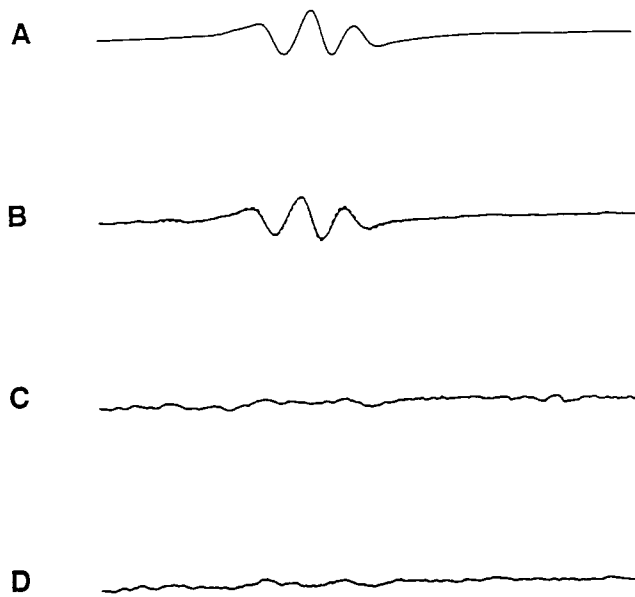


FIGURE 2 Additional analysis of the spectra of Fig. 1, showing that the spectra of active fibers can be deconvoluted into two components: one ordered as in rigor (20% of the total) and the other disordered as in relaxation (80% of the total). (A) 0.20 times rigor spectrum of Fig. 1 A. (B) Solid line, difference spectrum remaining after subtracting the disordered component from the spectrum of active fibers in 0 added  $P_i$ , pH 7.0 (Fig. 1 C minus 0.80 times Fig. 1 B). Dashed line, difference spectrum remaining after subtracting the disordered component from the spectrum of active fibers in 60 mM  $P_i$ , pH 6.2 (Fig. 1 D minus 0.80 times Fig. 1 B). The similarity of the ordered components, despite the shift of cross-bridges from force-producing states to pre-power-stroke states, shows that at least a portion of the pre-power-stroke states are ordered. The residual spectra for the above deconvolutions between active fibers are shown for pH 7, 0 added  $P_i$  (C) and for pH 6.2, 60 mM  $P_i$  (D). These spectra are flat to within experimental error. Thus there is no difference between the spectra from active fibers and a linear combination of spectra from rigor (20%) and relaxed (80%) fibers at both low and high  $[P_i]$ .

of the rigor spectrum and 80% of the relaxed spectrum are also given in Fig. 2 C (0  $P_i$ ) and Fig. 2 D (60 mM  $P_i$ ). To within experimental error, these spectra are both flat. Thus there is no difference between the spectra of active fibers and a linear spectral combination of 20% ordered (rigor) and 80% disordered (relaxed) at both low and high  $[P_i]$  for the spectra shown in Fig. 1. The 20% value for the active, ordered component is within the experimental envelope given in Table 1. Previous values for the active, ordered component have ranged between 12 and 20% (Thomas, 1987; Cooke et al., 1982; Fajer et al., 1990).

To investigate the effects of a wider variation in mechanical parameters, we varied both pH and  $[P_i]$ . Table 1 shows results obtained under four different conditions as pH and  $[P_i]$  were varied, singly and in combination. Isometric tension was decreased by either an increase in  $[P_i]$  or by a decrease in pH, with smaller changes occurring in stiffness. However, the same spectral decompositions were obtained when pH and  $[P_i]$  were varied separately, demonstrating that no new angular orientations were introduced under any of these conditions (spectra not shown). The proportional

changes in tension and stiffness as a result of increased  $[P_i]$  were approximately the same at both pH 7.0 and pH 6.2. Thus, although the exact states selectively populated by decreasing the pH are unknown, the data shown in Table 1 provide additional evidence that they may resemble those populated by increasing  $[P_i]$  both structurally and mechanically. In addition the data show that variation in pH does not affect our conclusions as regards variation in  $[P_i]$ .

The mechanical data shown in Table 1 were obtained on single fibers. To determine whether similar changes in tension occurred in the bundles of fibers observed in the EPR chamber, tension was measured in parallel experiments on a similar preparation as described in Materials and Methods. In the relaxed fiber bundle tension was low. Upon activation at pH 7 in the absence of added  $P_i$  the tension rose to a high value, which decreased rapidly by 65% upon subsequent activation in a high  $P_i$  solution at pH 6.2. This decrease in tension is similar to the 69% decrease observed in the single fibers. Although the absolute value of the tension is less certain here because of the difficulty in measuring an accurate diameter for the bundles, the tension was estimated to be  $0.15 \pm 0.015$  N/mm<sup>2</sup> in the pH 7 low  $P_i$  solution. This experiment shows that fibers in the capillary produce high tensions and that the effects of  $P_i$  are not masked by excessive build-up of  $P_i$  in the bundles. The results again argue that the mixing flow of the solution through the cell provides adequate perfusion of the fibers.

## DISCUSSION

The data obtained here show that probes attached to the reactive sulfhydryl on the catalytic domain remain ordered in the states populated by high  $P_i$  and  $H^+$ . Our probes are attached to the end of the cross-bridge catalytic domain furthest from actin and thus are in an ideal position to amplify any change in the orientation of the catalytic domain relative to the actin filament. We have used increased  $[P_i]$  and decreased pH to populate pre-power-stroke states. The probe spectra shown in Figs. 1 and 2 report that the catalytic domain maintains the same orientation in the pre-power-stroke states as it does in control active fibers. This shows that in these pre-power-stroke states, a cross-bridge spends at least a portion of its time with the catalytic domain ordered on actin. The same portion of cross-bridges are ordered, in fact, as are found at lower  $[P_i]$  and higher pH, where both the force and stiffness of the fibers are greater. Their orientation is the same as is seen for post-power-stroke, rigor, A-M cross-bridges. If the cross-bridges spend at least a portion of their time ordered in the pre-power-stroke state, and this orientation is the same as occurs at the end of the power stroke, one can conclude that the orientation of this domain did not change during the power stroke. Assuming that these states represent the pre-power-stroke structure in the model proposed by Rayment et al. (1993a), they support a key element of this model; i.e., the myosin catalytic domain remains rigidly oriented on the actin fila-

ment during the power stroke. If the catalytic domain does not move during the power stroke, the power stroke must be generated by the movement of another portion of the protein. As suggested by Rayment and co-workers (Rayment et al., 1993a), it appears likely that this movement involves the neck region of myosin. Indeed, several recent studies of spectroscopic probes support this conclusion, showing that the neck region is more disordered in active fibers than is the catalytic domain (Hambly et al., 1992) and that its orientation can be perturbed by force (Allen, Irving, and Goldman, unpublished observations).

The population of pre-power-stroke states can also be enhanced, transiently, after photolytic release of ATP from caged ATP, and the results obtained are compatible with our conclusion that some pre-power-stroke states are ordered. During the rise of tension that occurred after the release of ATP in rigor muscle fibers, the orientations of both fluorescent or paramagnetic probes attached to cys-707 did not change (Tanner et al., 1992; Roopnarine and Thomas, unpublished observation). These observations are fully consistent with the results found here. After binding of the liberated ATP to the myosin head, high concentrations of pre-power-stroke states will be achieved very rapidly. Thus the rise in force occurs upon the transition from non-force-generating, pre-power-stroke states to force-generating, power stroke states. The lack of a change in the probe spectra during this transition can be explained if the probe orientations in the pre-power-stroke states and the power stroke states are the same.

Our data suggest that at least a portion of the pre-power-stroke states obtained with high  $[P_i]$  are ordered; however, there is evidence that myosin heads can also bind to actin with disordered probes. States resembling those that follow ATP hydrolysis can be selectively populated by addition of 2,3-butanedione monoxime, a small molecule that binds to and stabilizes the  $A \cdot M \cdot ADP \cdot P_i$  state (Herrmann et al., 1992), or by the use of metallofluoride complexes of aluminum ( $AlF_x$ ) that function as a  $P_i$  analogue and stabilize an  $A \cdot M \cdot ADP \cdot AlF_x$  state (Chase et al., 1993). In contrast to the ordered probes that we find upon addition of high  $[P_i]$ , the spin probe spectra of the states that are stabilized by addition of 2,3-butanedione monoxime (Zhao et al., 1995) or  $AlF_x$  (Raucher and Fajer, 1994) display complete disorder, whereas mechanical stiffness remains high. An extensive line of investigation by Thomas and co-workers has shown that myosin heads bound to actin can be mobile on the microsecond time scale (Berger et al., 1989; Barnett and Thomas, 1989; Stein et al., 1990; Fajer et al., 1991; Berger and Thomas, 1993). In addition, electron cryomicroscopy has also provided evidence for attached, but randomly ordered cross-bridges (Hirose et al., 1993; Walker et al., 1994). Together, these data show that myosin cross-bridges are capable of binding to actin with disordered and/or mobile catalytic domains, although the position of these states in the cycle remains unclear.

Although there is no measurable decrease in the ordered fraction as  $[P_i]$  increases and pH decreases, the measured

stiffness has decreased. Fiber stiffness is often taken as a measure of the fraction of attached cross-bridges, suggesting that the fraction of attached cross-bridges has decreased without a decrease in the ordered fraction. Three different models, described below, could explain this apparent discrepancy. In model 1, the stiffness of the weakly bound states,  $A \cdot M \cdot ATP$  or  $A \cdot M \cdot ADP \cdot P_i$ , could be less than that of the strongly bound  $A \cdot M \cdot ADP$  states. This possibility was checked by simulations using a modified five-state cross-bridge model derived from that of Pate and Cooke (1986). The model was modified so that the stiffness of the weakly bound state, state 3 in the original model ( $A \cdot M \cdot ADP \cdot P_i$ ), is only one-half of that of the strongly bound states. As phosphate increases, the simulated decrease in tension is approximately twice that of the decrease in stiffness, with only a minor decrease in the fraction of attached cross-bridges, <5% detached at a tension decrease of 60%. Thus, a simple modification of existing models could explain the results, but unfortunately, the exact stiffness of the states populated by increased  $P_i$  is not known. In model 2, the attachment and detachment rates of the weakly bound states could be rapid. To appear as an ordered component in the EPR spectrum, the paramagnetic probe must remain ordered for only approximately 1  $\mu s$ . This is three orders of magnitude less than the time of the stiffness measurements, which require approximately 1 ms. In model 3, as discussed above, some heads may be attached to actin in states with disordered probes, and the changes in stiffness may arise from alterations within these states.

In summary, there are probably several weakly bound pre-power-stroke states with different properties. In the present work we show that at least a fraction of the states that are populated by elevated  $[P_i]$ , the physiological hydrolysis product, are ordered, showing that ordered states occur both before and after the power stroke. This result leads to the conclusion that the orientation of the cys-707 region, which is within the catalytic domain, does not change during the power stroke.

This work was supported by grants AR30868 (R.C.), AR42895 (R.C.), AR39643 (E.P.), and training grant 5T32CA09270 (L.Z.) from the USPHS. E.P. is an American Heart Association Established Investigator.

## REFERENCES

- Barnett, V. A., and D. D. Thomas. 1989. Microsecond rotational motion of spin-labeled myosin heads during isometric muscle contraction. *Biophys. J.* 56:517–523.
- Berger, C. L., E. C. Svensson, and D. D. Thomas. 1989. Photolysis of a photolabile precursor of ATP (caged ATP) induces microsecond rotational motions of myosin heads bound to actin. *Proc. Natl. Acad. Sci. USA.* 86:8753–8757.
- Berger, C. L., and D. D. Thomas. 1993. Rotational dynamics of actin-bound heads in active myofibrils. *Biochemistry.* 32:3812–3821.
- Chase, P. B., D. A. Martyn, M. J. Kushmerick, and A. M. Gordon. 1993. Effects of inorganic phosphate analogs on stiffness and unloaded shortening of skinned muscle fibers from rabbit. *J. Physiol.* 460:231–246.
- Cooke, R. 1986. The mechanism of muscle contraction. *CRC Crit. Rev. Biochem.* 21:53–118.

- Cooke, R., M. S. Crowder, and D. D. Thomas. 1982. Orientation of spin labels attached to cross-bridges in contracting muscle fibers. *Nature*. 300:776–778.
- Cooke, R., K. Franks, G. Luciani, and E. Pate. 1988. The inhibition of rabbit skeletal muscle contraction by hydrogen ions and phosphate. *J. Physiol.* 395:77–97.
- Fajer, P. G., E. A. Fajer, M. Schoenberg, and D. D. Thomas. 1991. Orientational disorder and motion of weakly attached cross-bridges. *Biophys. J.* 60:642–649.
- Fajer, P. G., E. A. Fajer, and D. D. Thomas. 1990. Myosin heads have a broad orientational distribution during isometric muscle contraction: time-resolved EPR studies using caged ATP. *Proc. Natl. Acad. Sci. USA*. 87:5538–5542.
- Fitts, R. H. 1994. Cellular mechanisms of muscle fatigue. *Physiol. Rev.* 74:49–94.
- Goldman, Y. E. 1987. Kinetics of the actomyosin ATPase in muscle fibers. *Annu. Rev. Physiol.* 49: 632–654.
- Hambly, B., K. Franks, and R. Cooke. 1992. Paramagnetic probes attached to a light chain on the myosin head are highly disordered in active fibers. *Biophys. J.* 63:1306–1313.
- Herrmann, C., J. Wray, F. Travers, and T. Barman. 1992. Effects of 2,3-butanedione monoxime on myosin and myofibrillar ATPase: an example of an uncompetitive inhibitor. *Biochemistry*. 31:12227–12232.
- Hibberd, M. A., J. A. Dantzig, D. R. Trentham, and Y. E. Goldman. 1985. Phosphate release and force generation in skeletal muscle fibers. *Science*. 228:1317–1319.
- Hibberd, M. A., and D. R. Trentham. 1986. Relationships between chemical and mechanical events during muscular contraction. *Annu. Rev. Biophys. Biophys. Chem.* 15:119–161.
- Hirose, K., T. D. Lenart, J. M. Murray, C. Franzini-Armstrong, and Y. E. Goldman. 1993. Flash and smash: rapid freezing of muscle fibers activated by photolysis of caged ATP. *Biophys. J.* 65:394–408.
- Metzger, J. M., and R. L. Moss. 1987. Greater hydrogen ion-induced depression of tension and velocity in skinned fibers of rat fast than slow muscle. *J. Physiol.* 393:727–742.
- Metzger, J. M., and R. L. Moss. 1990. Effects on tension and stiffness due to reduced pH in mammalian fast- and slow-twitch skinned muscle fiber. *J. Physiol.* 428:737–750.
- Pate, E., and R. Cooke. 1986. A model of cross-bridge action: the effects of ATP, ADP and  $P_i$ . *J. Muscle Res. Cell Motil.* 10:181–196.
- Pate, E., G. J. Wilson, M. Bhimani, and R. Cooke. 1994. Temperature dependence of the inhibitory effects of orthovanadate on shortening velocity in fast skeletal muscle. *Biophys. J.* 66:1554–1562.
- Raucher, D. and P. G. Fajer. 1994. Orientation and dynamics of myosin heads in aluminum fluoride induced pre-power-stroke states: an EPR study. *Biochemistry*. 33:11993–11999.
- Rayment, I., H. M. Holden, M. Whittaker, C. B. Yohn, M. Lorenz, K. C. Holmes, and R. A. Milligan. 1993a. Structure of the actin-myosin complex and its implications for muscle contraction. *Science*. 261: 58–65.
- Rayment, I., W. R. Rypniewski, K. Schmidt-Base, R. Smith, D. R. Tomchick, M. M. Benning, D. A. Winkelmann, G. Wesenberg, and H. M. Holden. 1993b. Three-dimensional structure of myosin subfragment-1: a molecular motor. *Science*. 261:50–57.
- Renaud, J. M., R. B. Stein, and T. Gordon. 1987. The effects of pH on force and stiffness development in mouse muscles. *Can. J. Physiol. Pharmacol.* 65:1798–1801.
- Schroder, R. R., D. J. Manstein, W. Jahn, H. Holden, I. Rayment, K. Helmong, and J. A. Spudich. 1993. Three dimensional atomic model of F-actin decorated with *Dictyostelium* myosin S1. *Nature*. 364:171–174.
- Seow, C. Y., and L. E. Ford. 1993. High ionic strength and low pH detain activated skinned rabbit skeletal muscle crossbridge in a low force state. *J. Gen. Physiol.* 101:487–511.
- Stein, R. A., R. D. Ludescher, P. S. Dahlberg, P. G. Fajer, R. L. Bennett, and D. D. Thomas. 1990. Time-resolved rotational dynamics of phosphorescent labeled myosin heads in contracting muscle fibers. *Biochemistry*. 29:10023–10031.
- Tanner, J. W., D. W. Thomas, and Y. E. Goldman. 1992. Transients in orientation of a fluorescent cross-bridge probe following photolysis of caged nucleotides in skeletal muscle fibers. *J. Mol. Biol.* 223:185–203.
- Taylor, E. W. 1977. Transient phase of adenosine triphosphate hydrolysis by myosin, heavy meromyosin and subfragment-1. *Biochemistry*. 16: 732–740.
- Thomas, D. D. 1987. Spectroscopic probes of muscle cross-bridge rotation. *Annu. Rev. Physiol.* 49:691–709.
- Thomas, D., and R. Cooke. 1980. Orientation of spin-labeled myosin heads in glycerinated muscle fibers. *Biophys. J.* 32:891–906.
- Walker, M., H. White, B. Belknap, and J. Trinick. 1994. Electron cryomicroscopy of acto-myosin-S1 during steady state ATP hydrolysis. *Biophys. J.* 66:1563–1572.
- Zhao, L., N. Naber, and R. Cooke. 1995. Muscle cross-bridges bound to actin are disordered in the presence of 2,3-butanedione monoxime. *Biophys. J.* 68:1980–1990.